Publishing Excellence Inspiring Progress
ARISTON PUBLICATIONS
Energy & Environment Advances
ISSN: xxxx-xxxx https://aristonpubs.com/energy-environment-advances https://doi.org/10.69626/eea.2024.0085

RESEARCH ARTICLE

Enhanced Performance of P3HT: PCBM Organic Solar Cells: Thickness Optimization and Recommendation Analysis

Iram Masood *, Mukesh Pratap Singh, Mohd Amir

ABSTRACT: Organic solar cells (OSCs) based on polymer-donor and fullerene-acceptor blends have garnered significant attention due to their cost-effectiveness, flexibility, and ease of fabrication. However, challenges such as low power conversion efficiency (PCE) and poor stability hinder their commercial viability. This study focuses on optimizing the thickness of various layers in a P3HT:PCBM-based OSC with the structure ITO/PEDOT:PSS/P3HT:PCBM/ZnSe/Al, employing OghmaNano simulation software. Additionally, non-geminate recombination effects and temperature stability were analyzed to understand their impact on device performance. The thickness of the active material (P3HT:PCBM) was varied between 100–300 nm, while transport and electrode layers were optimized to achieve balanced charge transport and effective light absorption. Our results demonstrate that the optimized structure achieved a PCE of 9.60%, with an open circuit voltage (VOC) of 0.64 V, a short circuit current density (JSC) of 206.70 A/m², and a fill factor (FF) of 72.13%. Moreover, recombination analysis revealed that mitigating non-geminate recombination could significantly enhance device performance. ZnSe was identified as an effective electron transport layer due to its transparency, favorable energy band alignment, and high electron mobility. This study highlights the importance of layer thickness optimization and recombination control in improving the efficiency and stability of OSCs. The findings pave the way for further advancements in OSC technology, potentially bridging the gap toward their commercialization.

Keywords: Organic solar cells, P3HT:PCBM, Bulk heterojunction, Thickness optimization, Recombination analysis.

Received: 06 March 2024; Revised: 18 April 2024; Accepted: 05 May 2024; Published Online: 21 May 2024

1. INTRODUCTION

The escalating global demand for energy, fueled by rapid industrialization and population growth, has necessitated the exploration of alternative energy sources to mitigate the issue of energy scarcity [1, 2]. Traditional energy generation methods, primarily dependent on fossil fuels, face significant challenges, including resource depletion, environmental pollution, and greenhouse gas emissions [3]. To address these challenges, renewable energy technologies such as solar energy have emerged as a promising solution. Among the various solar energy harvesting methods, flexible thin-film-based solar cells are gaining considerable attention due to their lightweight nature, adaptability, and potential for integration into unconventional surfaces [4, 5]. These advancements underscore the paradigm shift towards sustainable and innovative energy solutions.

In the realm of thin-film solar cells, organic bulk heterojunction (BHJ) solar cells represent a groundbreaking development. Unlike their silicon-based counterparts, organic solar cells (OSCs) offer unique advantages such as low-cost fabrication, mechanical flexibility, and lightweight architecture [6, 7]. These features make OSCs an ideal candidate for diverse applications, including wearable electronics, portable power devices, and building-integrated photovoltaics. Despite these advantages, the commercialization of OSCs is hindered by inherent limitations, primarily their relatively low power conversion efficiency (PCE) and stability under operational conditions [8, 9]. Addressing these challenges has become a focal point

Department of Applied Sciences & Humanities, Faculty of Engineering and Technology, Jamia Millia Islamia, New Delhi, India

* Author to whom correspondence should be addressed: iram188891@st.jmi.ac.in (Iram Masood)

of research within the scientific community, driving advancements in materials, device architecture, and optimization strategies.

Organic solar cells typically consist of a blend of electron-donating and electron-accepting materials, forming the active layer responsible for light absorption and charge generation. Among the widely studied material combinations, poly(3-hexylthiophene) (P3HT) serves as the electron-donating polymer, while [6,6]-phenyl-C61-butyric acid methyl ester (PCBM) functions as the electron acceptor [10, 11]. This P3HT:PCBM blend has become a model system for investigating the fundamental aspects of OSCs due to its well-defined molecular structure, ease of processing, and moderate efficiency [12]. However, achieving a high-performance OSC requires careful consideration of several critical factors, including active material thickness, transport layers (TLs) design, electrode configurations, energy level alignment, exciton dissociation, and charge transport dynamics [13]. These parameters play a pivotal role in determining the efficiency and stability of the device.

The optimization of OSC architecture has led to significant improvements in performance. One key approach involves the incorporation of transport layers, which facilitate efficient charge extraction and reduce energy losses [14]. The electron transport layer (ETL) and hole transport layer (HTL) are essential components in an OSC, as they ensure selective charge transport, suppress charge recombination, and establish energy barriers that prevent reverse current flow. The alignment of the lowest unoccupied molecular orbital (LUMO) and highest occupied molecular orbital (HOMO) energy levels between the active material and the transport layers is crucial for efficient charge transfer [15]. Moreover, the thickness and material properties of the TLs directly impact the optical and electrical performance of the device.

Various materials have been explored as transport layers in OSCs, each selected based on specific properties such as energy level alignment, charge mobility, and transparency [16]. Commonly used ETL materials include titanium dioxide (TiO_2), tungsten disulfide (WS_2), tungsten trioxide (WO_3), and zinc oxide (ZnO) [17, 18]. Similarly, HTL materials such as molybdenum trioxide (MoO_3), copper oxide (CuO), and PEDOT:PSS (poly(3,4-ethylenedioxythiophene):polystyrene sulfonate) have demonstrated favorable properties for OSC applications. However, zinc selenide (ZnSe) remains relatively underexplored as an ETL in OSCs, particularly in combination with P3HT:PCBM active layers [19]. ZnSe offers several advantages as an ETL material, including high optical transparency, excellent electron mobility, and well-aligned HOMO and LUMO energy levels with the active layer. These characteristics make ZnSe a promising candidate for enhancing OSC performance [20]. Additionally, PEDOT:PSS, a widely used HTL material, exhibits high hole mobility, good optical transparency, and suitable energy level alignment with the active layer. The synergy between ZnSe and PEDOT:PSS in OSCs has the potential to improve charge transport efficiency, reduce recombination losses, and enhance overall device performance [21, 22].

In this study, we investigate the use of ZnSe as an ETL in combination with PEDOT:PSS as an HTL to fabricate P3HT:PCBM-based OSCs. By leveraging the complementary properties of these materials, we aim to address the challenges of low PCE and stability in OSCs. Our research focuses on optimizing the thickness and energy level alignment of the transport layers, studying their impact on charge transport dynamics, and evaluating the resulting device performance. Furthermore, we explore the influence of ZnSe's material properties, including its transparency, electron mobility, and interfacial compatibility with the active layer, on the overall efficiency of the OSC. This work contributes to the growing body of knowledge on OSCs by demonstrating the potential of ZnSe as an effective ETL material and providing insights into the design and optimization of OSC architectures. By addressing the fundamental challenges associated with OSCs, our findings pave the way for the development of high-performance, stable, and cost-effective organic solar cells, advancing the prospects of renewable energy technologies for a sustainable future.

2. DEVICE ACHITECHURE AND SIMULATION DETAILS

2.1. Device Structure and Energy Alignments

In this work we have simulated P3HT:PCBM based conventional organic solar cell with the device structure that consist of ZnSe, PEDOT:PSS, Indium tin oxide (ITO) and Aluminium (Al) as ETL, HTL, anode and cathode respectively. The stack of all layers in OSC is in the sequence, i.e. ITO/PEDOT:PSS/P3HT:PCBM/ZnSe/Al. P3HT:PCBM based OSC has received considerable interest, in both conventional and inverted configurations with PEDOT:PSS as HTL. The electron affinity (-2.9 eV) of PEDOT:PSS aligns with the LUMO (-3.8 eV) of active layer in such a way that creates an energy barrier for electrons. The minimum energy off-set between LUMO of P3HT:PCBM (-3.8 eV) and LUMO of ZnSe (-4.09 eV) allows effective electron transfer to cathode while its HOMO (- 6.9 eV) consist of large offset with active layer's HOMO (-4.9 eV), blocking hole transfer to the cathode. All the materials except ZnSe, are taken from OghmaNano material database. The material optical constants for ZnSe are taken from reference [11]. The initial device thickness is 100 nm, 20 nm, 170 nm, 10 nm, and 100 nm for ITO, PEDOT:PSS, P3HT:PCBM, ZnSe and Al respectively. The Schematic diagram of studied device structure is presented in Figure 1(a). The diagram of energy band alignment of materials in device is shown in Figure 1(b).

2.2. Description of OghmaNano Simulation Model

The "Organic and hybrid material nano" (OghmaNano) is an open access simulation software that supports general

purpose modelling of photovoltaic devices and other devices such as Organic Field Effect Transistors, Organic Light Emitting Diodes and devices related to optics and electronics. The OghmaNano simulator has been used in obtaining all the results in this work. The snap-shot of simulated device structure is presented in Figure 1(c).The poisson equation, drift-diffusion equations and the current continuity equations for the charge carriers are numerically executed in electrical model of the program [12-14].The conduction band i.e. LUMO and valance band also called HOMO of the active material in the program is defined using relation (1) and (2), respectively. The expression for potential distribution (φ) within OSC is governed by relation (3), which is also known as Poisson's equation:

$$E_{LUMO} = -\chi - q\varphi \quad (1)$$

$$E_{HOMO} = -\chi - E_G - q\varphi \quad (2)$$

$$\frac{d}{dx}\varepsilon_0\varepsilon_r\frac{d\varphi}{dx} = q\left(n_f - p_f + n_t - p_t\right) \quad (3)$$

Where, the permittivity of free space is represented by ε_0 and ε_r expresses the relative permittivity of active material. The values nf /pf denotes free electron/hole density and nt /pt defines trapped electron/hole densities. The drift and diffusion processes are governed by (4), (5) and continuity equations are given as (6), (7):

$$J_n = \mathrm{q}\mu_e\ \mathrm{n}_f\frac{\partial E_{LUMO}}{\partial \mathrm{x}} + \mathrm{q}D_e\frac{\partial n_f}{\partial x} \quad (4)$$

$$J_p = \mathrm{q}\mu_p\ \mathrm{p}_f\frac{\partial E_{HOMO}}{\partial \mathrm{x}} + \mathrm{q}D_h\frac{\partial p_f}{\partial x} \quad (5)$$

$$\frac{\partial J_n}{\partial \mathrm{x}} = \mathrm{q}(R_e - G) \quad (6)$$

$$\frac{\partial J_p}{\partial \mathrm{x}} = \mathrm{q}(R_h - G) \quad (7)$$

Where J_n /J_p are electron/hole current densities and De /Dh show diffusion coefficients of electron /hole. The rate of generation for free electrons or holes is shown as G and R(e/h) is the total recombination.

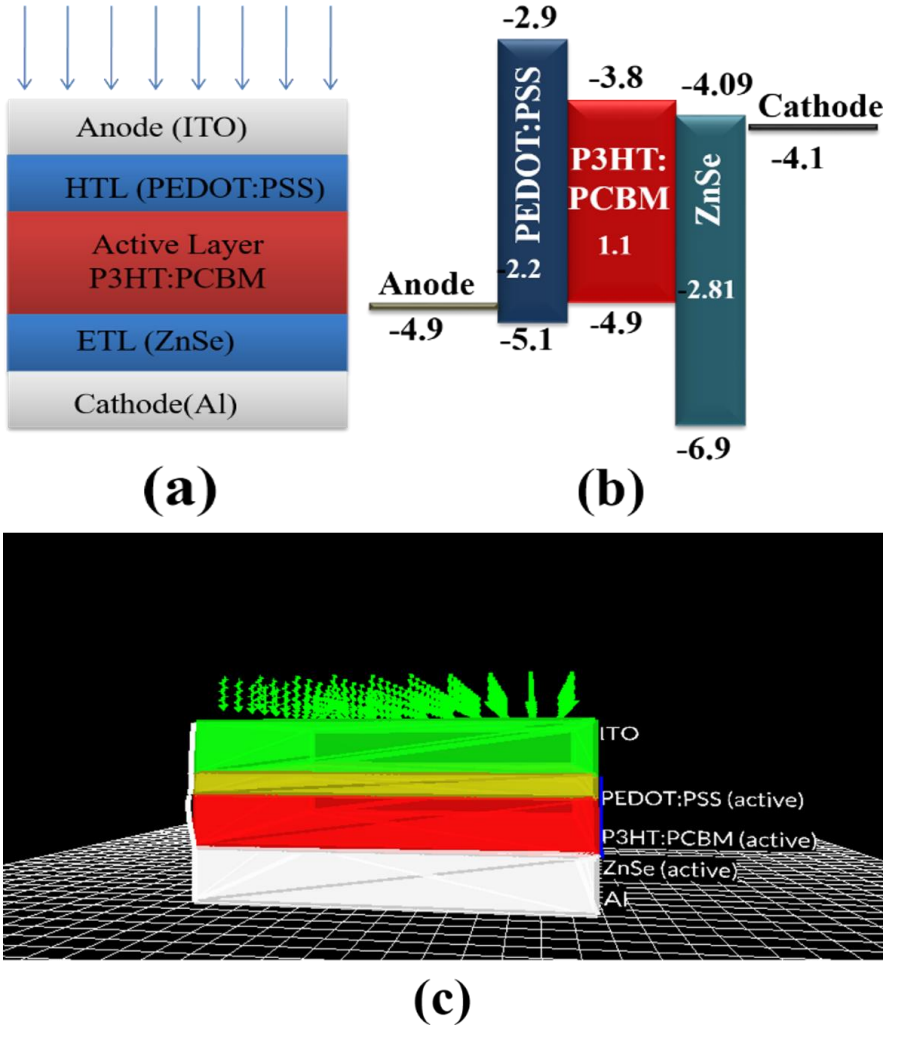

Fig. 1. (a) The device structure of OSC (b) Energy band alignments of used materials (c) Snapshot of simulated device from OghmaNano software.

Table 1. Density of states parameters for active material.

Simulation parameters of P3HT:PCBM	Values
Density of trapped electron (m^{-3} eV^{-1})	3.8×10^{26}
Density of trapped hole (m^{-3} eV^{-1})	1.45×10^{25}
Tail slope of electron (eV)	0.04
Tail slope of hole (eV)	0.06
Electron Mobility (m^2 V^{-1} s^{-1})	2.48×10^{-7}
Hole Mobility (m^2 V^{-1} s^{-1})	2.48×10^{-7}
Relative permittivity of active material	3.8
Number of traps (bands)	20
Free electron to trapped electron (m^{-2})	2.5×10^{-20}
Trapped electron to free hole (m^{-2})	1.32×10^{-22}
Trapped hole to free electron (m^{-2})	4.67×10^{-26}
Free hole to trapped hole (m^{-3})	4.86×10^{-22}
Effective density of states for free electron (m^{-3})	1.28×10^{27}
Effective density of states for free hole (m^{-3})	2.86×10^{25}
Affinity of Electron (eV)	3.8
Energy gap (eV)	1.1

Table 2. Simulation Parameters used for ETL and HTL.

Name	PEDOT:PSS [17]	ZnSe [18]
Electron affinity (eV)	2.9	4.09
Band gap (eV)	2.2	2.81
Relative permittivity	3	8.6
Effective DOS in conduction band (m^{-3})	2.2×10^{21}	2.2×10^{24}
Effective DOS in valance band (m^{-3})	1.8×10^{24}	1.8×10^{24}
Electron mobility (m^2 V^{-1} s^{-1})	2×10^{-6}	2.5×10^{-3} [19]
Hole mobility (m^2 V^{-1} s^{-1})	2×10^{-8}	1×10^{-2} [19]

The OghmaNano software applys Shockley-Read-Hall recombination model to find the charge carrier trapping and recombination, moreover to simulate the optical aspects of the device transfer matrix method is executed [13, 14]. The material parameters for active layer and transport layers are given in Table 1 and Table 2, respectively.

3. RESULTS AND DISCUSSION

3.1. Thickness Optimization

Improving the power conversion efficiency of solar cells depends on their specific characteristics. These characteristics parameters primarily include the open circuit voltage (V_{OC}), short circuit current density (J_{SC}) and *FF.* The value of J_{SC} depends on electron-hole pair generation during exposure to light and charge separation capability. The *Jsc* can be adjusted by either altering the device materials or changing the thickness of the layer stack. The thickness of materials impacts the power conversion efficiency of OSC. We have altered the material thicknesses of the proposed OSC device and analyzed variations in device electrical parameters accordingly.

Role of Active Layer Thickness: Active material is the most significant component of an organic solar cell since it generates excitons in response to light absorption and effects the electrical parameters of OSC. The thickness of active material (P3HT:PCBM) has been changed from 100 nm to 300 nm to investigate the variation in related characteristic parameters. Figure 2(a) depicts the acquired characteristic parameters with variation in active layer thickness. The short circuit current density (*JSC*) depends on the light absorption and charge carrier generation, very thin layer of active material does not facilitate effective photon to electron generation due to minimum material available for light absorption resulting in low J_{SC} values. The thicker active layer shows increase in J_{SC} but it also increases the series resistance of the device which degrades the Fill Factor (*FF*) which is clearly depicted in Figure 2(a). The thickness change has a very small impact on the open circuit voltage (V_{OC}), which is determined by the energy difference between the HOMO of P3HT (donor) and the LUMO of PCBM (acceptor),

it cannot exceed beyond that limit. The results reveal that as the thickness changes from 100 nm to 300 nm, first short circuit current density (J_{SC}) changes from 203.90 A/m^2 to 198.96 A/m^2 then J_{SC} increases as thickness goes beyond 170 nm due to more photon to charge carrier generation in the active material but at the same time excess of generated charge carriers also go through recombination, decreasing power conversion efficiency (*PCE*). Also the increase in thickness degrades the *FF* due to series resistance increment. The *PCE* of OSC is govern by the relation (8) [2]. Considering the PCE dependency from equation (8), we have taken the combined role of *Voc*, J_{SC} and *FF* to determine the optimized thickness of active layer which turned out 100 nm, resulting in 9.44% PCE for the studied structure. The current-voltage characteristics for active material is depicted in Figure 2 (d). The power conversion efficiency can be calculated from the below equation:

$$PCE\ (\eta) = \frac{V_{OC} \times J_{SC} \times FF}{P_{in}} \quad (8)$$

Role of Transport Layer Thicknesses: The results obtained from change in transport layer thicknesses are plotted in Figure 2 (b) and (c). The current-voltage characteristics for transport material namely, HTL and ETL are given in Figure 2 (e) and (f), respectively. The thickness of HTL(PEDOT:PSS) plays an important role in extracting charge carriers, as HTL acts like a spacer between anode and active material transmitting light through it.

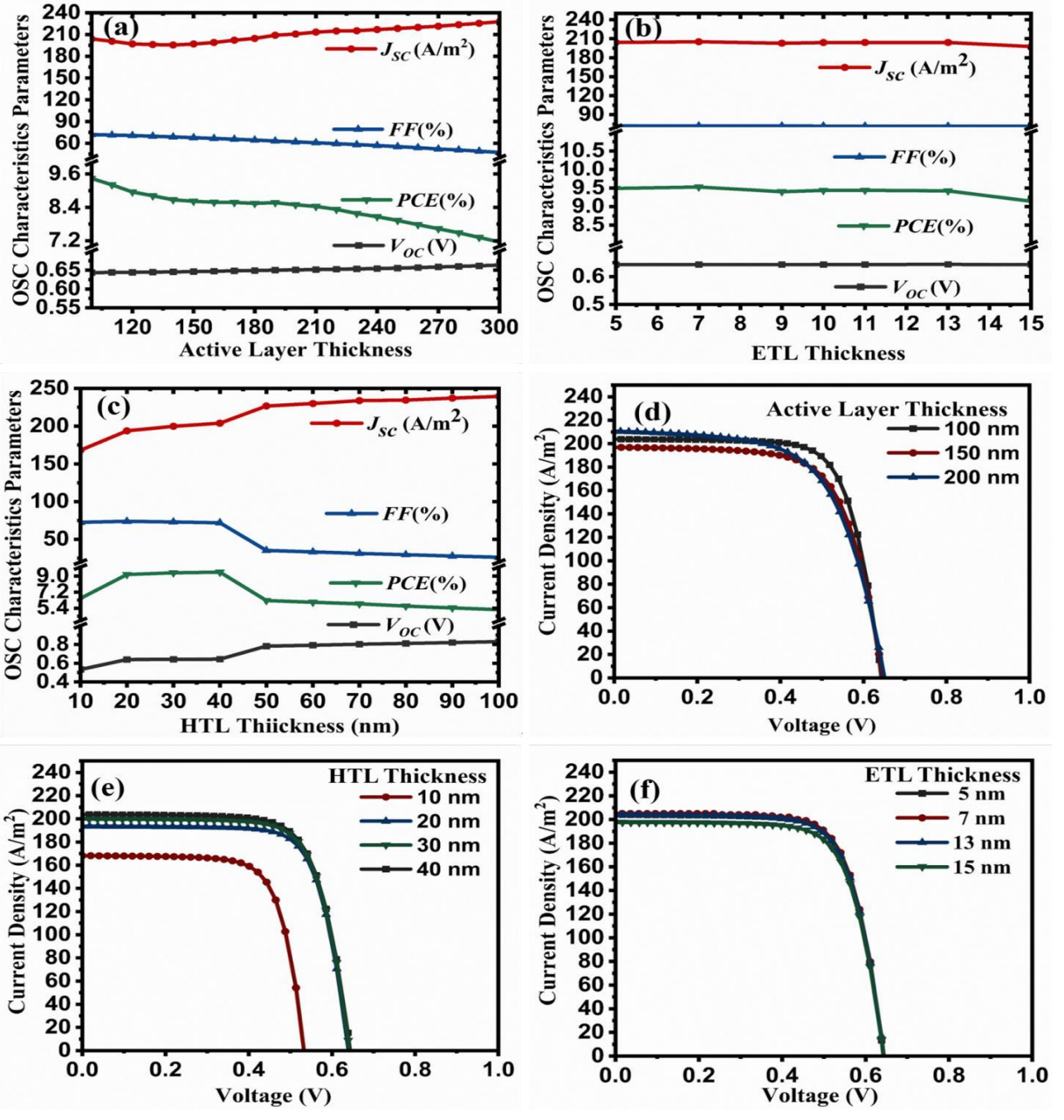

Fig. 2. The electrical parameters (*VOC*, *JSC*, FF, PCE) effected by change in: (a) Active material thickness (b) ETL thickness (c) HTL thickness and Current versus voltage characteristics at different layer thicknesses: (d) Active layer, and (e) HTL (f) ETL.

Figure 2(c) shows that *JSC* contributes in enhancement of PCE due to good transmission of light through PEDOT:PSS enhancing photon harvesting. The result shows HTL thickness impacts J_{SC} and *FF.* The increment in thickness reduces the *PCE* from 9.44% to 5.23%. The possible cause behind this reduction is the increment in series resistance of the OSC, deducting *FF*. The change in all electrical parameters are considered and the best *PCE* is obtained as 9.44% for 40 nm thick HTL.

The ETL thickness versus characteristic parameters are shown in Figure 2(b). The slightly decreased *PCE* is due to the possibility of recombination. A thick ETL facilitates the longer path for charge carrier promoting recombination loss before charge extraction at cathode. The low energy offset between ZnSe ETL and Al boost electron collection to cathode. The thicker ETL (15 nm) results in 9.14% *PCE* while at optimized thickness (7 nm) the attained *PCE* is 9.53%.

Role of Electrode Thicknesses: Indium Tin Oxide based anode are most widely used in solar cells due to their crucial role in improving device output [15, 16]. We have selected ITO as anode in our device due to its transparency and work function matching with the PEDOT:PSS. The low energy off-set of ITO and PEDOT:PSS are reason for efficient hole collection at anode. On the other hand, energy off-set between work function of Al (-4.7 eV) and ZnSe LUMO plays significant role in negative charge collection at cathode. The thickness of ITO and Al is changed from 50-100 nm and the results are plotted in Figure 3 (a) and (b). It has been noted that thin ITO films show significant change in *JSC* as the transmission of light is good at lower thicknesses. Also this results in higher charge generation rates in active material. The results in Figure 3 (a) and (b) show that *PCE* is 9.58% at 50 nm thick anode while increasing the thickness lowers the *PCE* to 9.46%. The cathode's thickness, when increased, slightly affects the *PCE.* At 50 nm *PCE* drops to 9.53% but at higher thicknesses *PCE* increases. The back reflection of light from metal cathode to active material at different thicknesses also impacts the *PCE*. The best *PCE* obtained is 9.59% at 90 nm thick cathode. The current-voltage curves for anode and cathode thicknesses are plotted in Figure 3 (c) and (d), respectively.

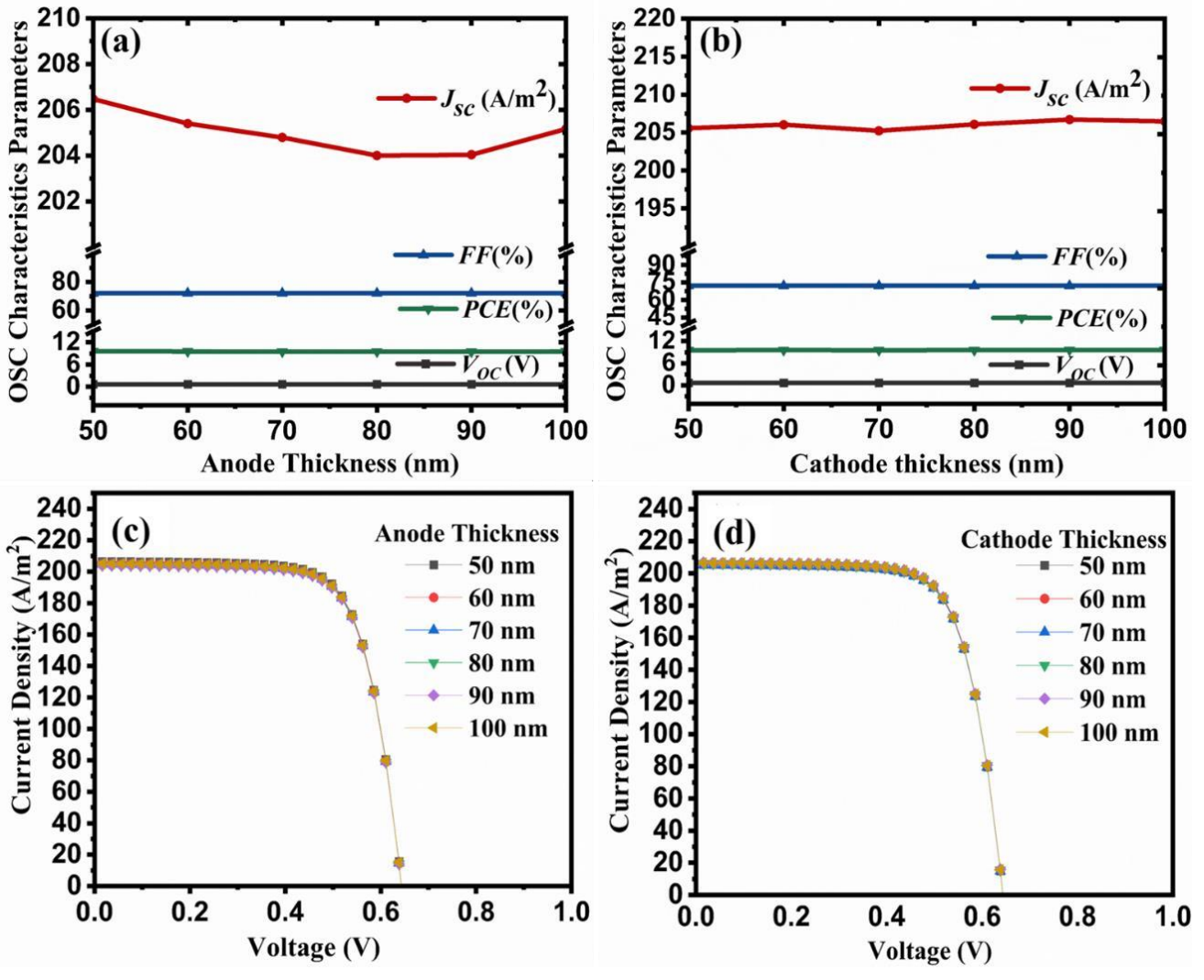

Fig. 3. The electrical parameters (VOC, JSC, FF, PCE) effected by variation in: (a) Anode thickness (b) Cathode thickness and Current versus voltage characteristics at different thicknesses: (c) Anode, and (d) Cathode.

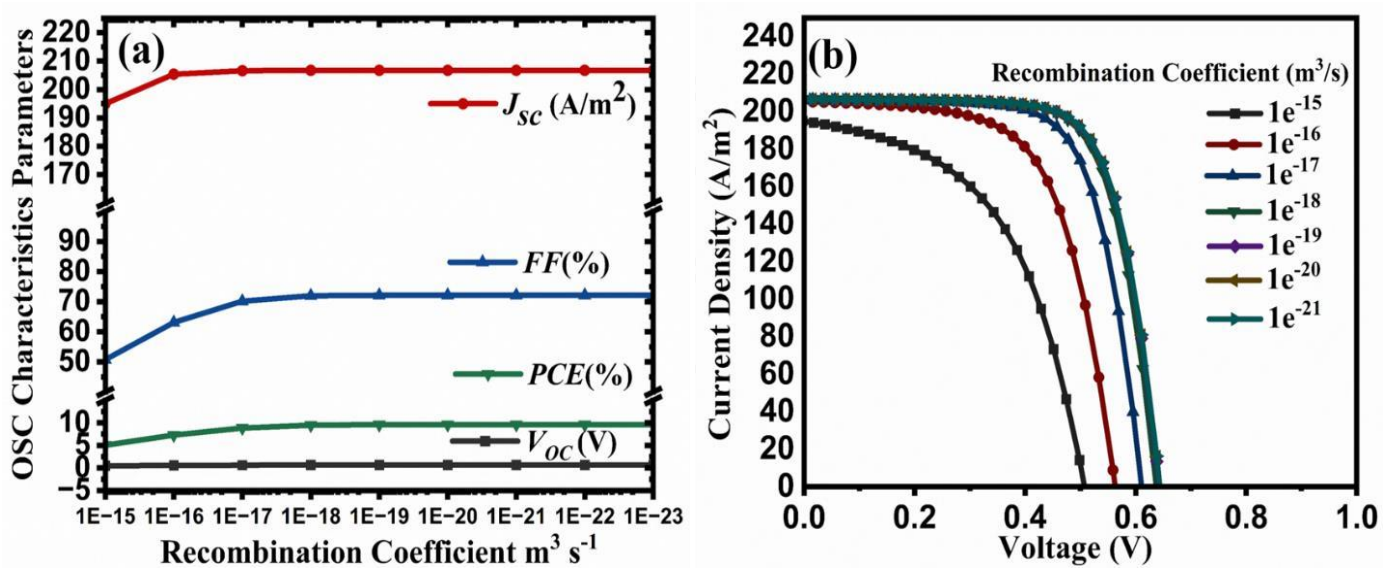

Fig. 4. The role of recombination coefficient (k) on (a) Electrical parameters and (b) Current-voltage characteristics of OSC.

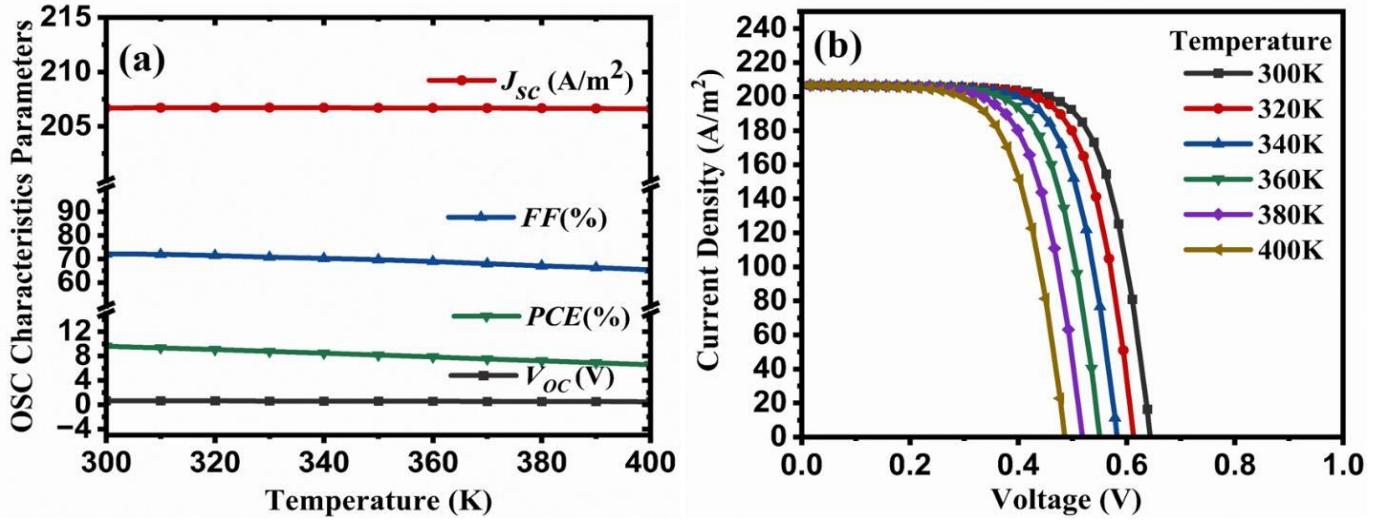

Fig. 5. The role and influence of temperature on: (a) the OSC characteristics parameters and (b) current voltage curves of OSC.

3.2. Recombination Analysis

Photo-induced charges (excitons) goes through separation at charge transfer states. These states either separates the excitons or they recombine. If the two random photon-induced and separated charges meets and recombine at the donor-acceptor interface, then this process is stated as non-geminate recombination. The results depicted in Figure 4 (a) shows the role of non-geminate recombination and current-voltage curves are plotted in Figure 4 (b). The results show that at lower values of recombination coefficient (k), *JSC* is significantly high, which indicates low free to free career recombination and efficient charge collection at electrodes At 1e^{-15} m^3/s value of k the lowest *PCE* (5.02%) is obtained showing a drop in *JSC*. At high recombination coefficient values, the low concentration of free charge carriers indicates the domination of non-geminate recombination. The *PCE* of 9.60% is obtained at the lower value of k, i.e. 1e^{-21} m^3/s. Other OSC parameters such as *FF* and *VOC* are not affected at varied values (1e^{-18} to 1e^{-23} m^3/s) of K.

3.3. Role of Temperature

The changes seen in OSC parameters (*JSC, VOC, FF*, and *PCE*) in Figure 5 (a), are caused by increase in temperature (T). The temperature has been risen from 300 K to 400 K to study its influence on OSC parameters.

Table 3. Electrical parameters of different OSC architecture reported in the literature.

V_{OC} (V)	J_{SC} (mA/cm^2)	FF (%)	PCE (%)	Ref.
0.59	15.21	45.50	4.07	[20]
0.55	19.8	50.00	5.30	[21]
0.66	12.01	59.00	4.65	[4]
0.34	7.58	56.50	2.13	[22]
0.61	13.20	64.08	5.46	[12]
0.64	20.67	72.13	9.60	This work

Table 4. Initial versus optimized device parameters.

ITO/PEDOT:PSS/P3HT:PCBM/ZnSe/Al				
Parameters	V_{OC} (V)	J_{SC} (mA/cm^2)	*FF* (%)	*PCE* (%)
Initial Device	0.54	199.05	68.79	7.44
Optimized Device	0.64	206.71	72.13	9.60

The simulation results show noteworthy changes occurs in *Voc, FF* and *PCE*. The drop in *VOC* from 64.35 V to 48.56 V, in *FF* from 72.13% to 65.39% and in PCE from 9.60% to 6.56% has been obtained. A slight variation in *Jsc* is obtained due to thermally generated charge carriers with rise in temperature. The dropping in *Voc* is caused by increase in saturation current and *PCE* goes low with increasing temperature, due to recombination triggered by thermally generated charge carriers. Since the rate of decrease in *VOC,* and *FF* over shadows the slight increment in *JSC*. The overall effect of OSC characteristic parameters is considered in results and Figure 5 (a) and (b) show the best operating temperature is 300K for stable working of OSCs.

The study focuses on simulating and optimizing the thickness of layers in a P3HT:PCBM-based bulk heterojunction organic solar cell (BHJ-OSC) with the structure "ITO/PEDOT:PSS/P3HT:PCBM/ZnSe/Al." The optimization process aimed to enhance the overall performance of the device. Table 3 presents a comparative analysis of the optimized OSC's power conversion efficiency (PCE) with values reported in the literature. The electrical parameters of the simulated OSC were analyzed under varying thicknesses, temperatures, and non-geminate recombination rates. The findings demonstrate that optimizing the thickness of all layers in the device significantly improves OSC efficiency. The optimized thickness values were determined to be 100 nm for the active layer (P3HT:PCBM), 40 nm for the hole transport layer (PEDOT:PSS), 7 nm for the electron transport layer (ZnSe), 50 nm for the anode (ITO), and 90 nm for the cathode (Al).

These optimized values are detailed in Table 4 and visually represented in Figure 6. Furthermore, the results revealed a degradation in OSC performance with increasing temperature and free charge carrier recombination. The ideal operating temperature for optimal performance was identified as 300 K. The comparative results, as shown in Table 4 and Figure 10, highlight that further improvements in power conversion efficiency can be achieved by carefully optimizing the device's layer thickness.

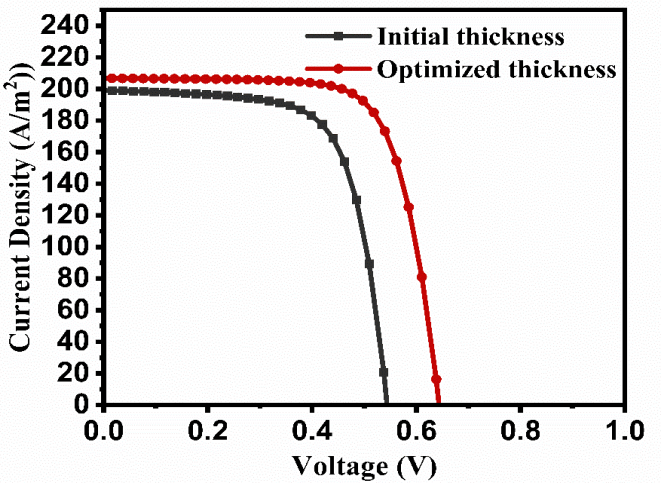

Fig. 6. The current versus voltage curves for initial and final device thickness.

4. CONCLUSION

The optimization of layer thicknesses in organic solar cells (OSCs) plays a pivotal role in enhancing their power conversion efficiency (PCE) and overall performance. In this work, we investigated the performance of a P3HT:PCBM-based OSC with the structure ITO/PEDOT:PSS/ P3HT:PCBM/ZnSe/Al, using Oghma-Nano simulation software. By systematically varying the thickness of the

active material, transport layers, and electrodes, we observed significant improvements in critical device parameters, including open circuit voltage (VOC), short circuit current density (JSC), and fill factor (FF). The optimized device exhibited a PCE of 9.60%, which is a substantial improvement for OSCs. This enhancement can be attributed to the efficient light absorption and exciton generation within the optimized active material thickness range (170 nm). Furthermore, the ZnSe electron transport layer contributed to the efficient collection of electrons at the cathode due to its suitable energy band alignment and high electron mobility. The hole transport layer, PEDOT:PSS, effectively facilitated hole extraction while blocking electron recombination at the anode. Non-geminate recombination analysis revealed that recombination significantly impacts PCE, particularly under suboptimal conditions. Temperature stability studies showed that the device maintained performance within acceptable limits, suggesting improved stability compared to conventional OSCs. These findings underscore the importance of comprehensive optimization strategies, including material selection, energy band alignment, and thickness tuning, to achieve higher efficiencies and stability in OSCs. Future studies should focus on integrating alternative transport layer materials and advanced device architectures to further enhance performance. This work provides valuable insights into overcoming efficiency and stability barriers in OSCs, paving the way for their practical applications in sustainable energy solutions.

DECLARATIONS

Ethical Approval

We affirm that this manuscript is an original work, has not been previously published, and is not currently under consideration for publication in any other journal or conference proceedings. All authors have reviewed and approved the manuscript, and the order of authorship has been mutually agreed upon.

Funding

Not applicable

Availability of data and material

All of the data obtained or analyzed during this study is included in the report that was submitted.

Conflicts of Interest

The authors declare that they have no financial or personal interests that could have influenced the research and findings presented in this paper. The authors alone are responsible for the content and writing of this article.

Authors' contributions

All authors contributed equally in the preparation of this manuscript.

ACKNOWLEDGEMENTS

Ms. Iram Masood would like to express her gratitude to the University Grants Commission (UGC) for providing the Non-NET fellowship. The Authors are thankful to Mr. Roderick C. I. Mackenzie for providing free access to OghmaNano.

REFERENCES

[1] Bernardo, G., Lopes, T., Lidzey, D.G. and Mendes, A., **2021.** Progress in upscaling organic photovoltaic devices. *Advanced Energy Materials*, 11(23), p.2100342.

[2] Zidan, M.N., Ismail, T. and Fahim, I.S., **2021.** Effect of thickness and temperature on flexible organic P3HT: PCBM solar cell performance. *Materials Research Express*, *8*(9), p.095508.

[3] Bonasera, A., Giuliano, G., Arrabito, G. and Pignataro, B., **2020.** Tackling performance challenges in organic photovoltaics: An overview about compatibilizers. *Molecul*es, 25(9), p.2200.

[4] Shaban, M., Benghanem, M., Almohammedi, A. and Rabia, M., **2021.** Optimization of the active layer P3HT: PCBM for organic solar cell. *Coatings*, 11(7), p.863.

[5] Husen, M.J., Aga, F.G. and Dibaba, S.T., **2023**. Theoretical Performance Analysis of Inverted P3HT: PCBM Based Bulk Hetero-Junction Organic Solar Cells through Simulation. *Advances in Materials Science and Engineering*, 2023(1), p.4204298.

[6] Davis, D., Shamna, M.S., Nithya, K.S. and Sudheer, K.S., **2022**, July. Graphene as a hole transport layer for enhanced performance of P3HT: PCBM bulk heterojunction organic solar cell: a numerical simulation study. *In IOP Conference Series: Materials Science and Engineering* (Vol. 1248, No. 1, p. 012011). IOP Publishing.

[7] Masood, I., Singh, M.P. and Amir, M., **2023,** February. Analysis of Different Layers Thicknesses on the Performance of Organic Solar Cells. In 2023 *International Conference on Power, Instrumentation, Energy and Control* (PIECON) (pp. 1-5). IEEE.

[8] Amir, M., Singh, M.P. and Masood, I., **2022,** November. Recombination Analysis of $CH_3NH_3PbI_3$ Perovskite

Solar Cell for Optimized Device Structure. In International Conference on Nanotechnology: Opportunities and Challenges (pp. 465-469). Singapore: Springer Nature Singapore.

[9] Hossain, M.K., Toki, G.I., Kuddus, A., Rubel, M.H.K., Hossain, M.M., Bencherif, H., Rahman, M.F., Islam, M.R. and Mushtaq, M., **2023.** An extensive study on multiple ETL and HTL layers to design and simulation of high-performance lead-free $CsSnCl_3$-based perovskite solar cells. Scientific Reports, 13(1), p.2521.

[10] Valeti, N.J., Prakash, K. and Singha, M.K., **2023.** Numerical simulation and optimization of lead free $CH_3NH_3SnI_3$ perovskite solar cell with $CuSbS_2$ as HTL using SCAPS 1D. *Results in Optics*, *12*, p.100440.

[11] Loewenstein, E.V., Smith, D.R. and Morgan, R.L., **1973.** Optical constants of far infrared materials. 2: Crystalline solids. *Applied Optics*, *12*(2), pp.398-406.

[12] Abdallaoui, M., Sengouga, N., Chala, A., Meftah, A.F. and Meftah, A.M., **2020.** Comparative study of conventional and inverted P3HT: PCBM organic solar cell. *Optical Materials*, 105, p.109916.

[13] MacKenzie, R.C., **2022**. Gpvdm user manual v7. 88.

[14] MacKenzie, R.C., Shuttle, C.G., Chabinyc, M.L. and Nelson, J., **2012.** Extracting microscopic device parameters from transient photocurrent measurements of P3HT: PCBM solar cells. A*dvanced Energy Materials*, 2(6), pp.662-669.

[15] Sousa, M.G. and Da Cunha, A.F., **2019.** Optimization of low temperature RF-magnetron sputtering of indium tin oxide films for solar cell applications. *Applied Surface Science*, 484, pp.257-264.

[16] Amalathas, A.P. and Alkaisi, M.M., **2016.** Effects of film thickness and sputtering power on properties of ITO thin films deposited by RF magnetron sputtering without oxygen. *Journal of Materials Science: Materials in Electronics*, 27, pp.11064-11071.

[17] Liu, X., Yan, K., Tan, D., Liang, X., Zhang, H. and Huang, W., **2018.** Solvent engineering improves efficiency of lead-free tin-based hybrid perovskite solar cells beyond 9%. *ACS Energy Letters*, 3(11), pp.2701-2707.

[18] Moiz, S.A., Alzahrani, M.S. and Alahmadi, A.N., **2022.** Electron transport layer optimization for efficient PTB7: PC70BM bulk-heterojunction solar cells. *Polymers*, 14(17), p.3610.

[19] Et-taya, L., Benami, A. and Ouslimane, T., **2022.** Study of CZTSSe-based solar cells with different ETMs by SCAPS. *Sustainability*, 14(3), p.1916.

[20] Hamed, M.S. and Mola, G.T., **2019**. Copper sulphide as a mechanism to improve energy harvesting in thin film solar cells. *Journal of Alloys and Compounds*, 802, pp.252-258.

[21] Mbuyise, X.G. and Mola, G.T., **2020**. Polycrystal metals nano-composite assisted photons harvesting in thin film organic solar cell. *Solar Energy*, 208, pp.930-936.

[22] Guerrero, A., Boix, P.P., Marchesi, L.F., Ripolles-Sanchis, T., Pereira, E.C. and Garcia-Belmonte, G., **2012.** Oxygen doping-induced photogeneration loss in P3HT: PCBM solar cells. *Solar Energy Materials and Solar Cells,* 100, pp.185-191.

